

PEARL

Metals in boat paint fragments from slipways, repair facilities and abandoned vessels: An evaluation using field portable XRF

Comber, Sean

Published in:
Talanta

DOI:
[10.1016/j.talanta.2014.08.012](https://doi.org/10.1016/j.talanta.2014.08.012)

Publication date:
2015

Link:
[Link to publication in PEARL](#)

Citation for published version (APA):

Comber, S. (2015). Metals in boat paint fragments from slipways, repair facilities and abandoned vessels: An evaluation using field portable XRF. *Talanta*, 0(0), 372-378. <https://doi.org/10.1016/j.talanta.2014.08.012>

All content in PEARL is protected by copyright law. Author manuscripts are made available in accordance with publisher policies. Wherever possible please cite the published version using the details provided on the item record or document. In the absence of an open licence (e.g. Creative Commons), permissions for further reuse of content should be sought from the publisher or author.

Metals in boat paint fragments from slipways, repair facilities and abandoned vessels: an evaluation using field portable XRF

**Andrew Turner*, Sean Comber, Aldous B. Rees, Dimitrios Gkiokas,
Kevin Solman**

School of Geography, Earth and Environmental Sciences

Plymouth University

Drake Circus

Plymouth PL4 8AA

UK

*Corresponding author. Tel: +44 1752 584570; Fax: +44 1752 584710; e-mail: aturner@plymouth.ac.uk

Abstract

Paint flaking off abandoned vessels or generated during boat repair is hazardous to human health and wildlife. In this study, a means of screening paint fragments using a field portable-X-ray fluorescence (FP-XRF) spectrometer is described. The technique is capable of delivering rapid, surficial measurements of Ba, Cu, Pb and Zn down to concentrations less than $150 \mu\text{g g}^{-1}$, and Sn and Cr to concentrations of a few hundred $\mu\text{g g}^{-1}$. Application of the technique to fragments collected from slipways, yards, hardstandings, abandoned boats and ships undergoing maintenance throughout the EU reveal highly variable concentrations of metals among samples from the same environment or from the same region of a given boat; in many cases, variability is also evident in different areas or on different surfaces of the same fragment. Of particular concern are elevated concentrations of substances that have been restricted or banned (e.g. Sn, an indicator of organotin, up to concentrations of 4%, and Pb up to concentrations of 20%). Although FP-XRF can rapidly inspect samples whose composition and origin are unknown and can assist in instantaneous decision making, a full risk assessment will rely on additional analyses of the precise species (e.g. organo- forms) of the metals present.

Keywords: *boat paints; FP-XRF; ICP-MS; metals; contamination; antifouling*

1. Introduction

Because of the harsh and aggressive conditions that boats and ships are exposed to, many specialist paints are required with high corrosion protection [1]. Such paints include those that provide protection to steel hulls, boat-toppings and topsides, those that inhibit the biofouling of the hull, and blast primers and tie-coats. More conventional primers, undercoats and enamels are generally used internally and for the topsides of smaller boats.

The various functions and colours of boat paints are engendered by the addition of a variety of different chemical components with particular properties. Given that many of these components, like pigments, biocides, dryers and extenders, may be metal-based, boat paints pose a threat to human health and to wildlife if not managed properly. The greatest hazard arises when paint layers are removed during boat maintenance, repair or repainting because of the generation of fragments and dusts from sanding, blasting, scraping and chipping [2]. In commercial and military shipyards, paint waste is usually contained and disposed of safely [3,4]. The maintenance of smaller craft in boatyards or on slipways and hardstandings is unregulated, however, and despite boaters being asked to comply with voluntary codes of practice, and in particular those related to the disposal of antifouling formulations [5,6], accumulations of paint waste are commonly observed at these facilities. Paint particles are readily transported to (or even swept into) surrounding soils and sediments where metal contamination is often reported [7,8].

Another means by which paint particles may be introduced in to the environment is through the weathering and erosion of paint layers on abandoned boats and ships. Abandoned vessels of various ages and states of dereliction are commonplace on the

shores of rivers, estuaries and coasts, but appear to be exempt from any kind of direct or enforceable environmental regulation [9]. With respect to the potential for local metal contamination, older boats are of particular concern because flaking paint may contain substances that have been restricted or banned since their original application.

Because of the environmental risks and health hazards associated with high quantities of metals in boat paints there is a need for rapid and accurate chemical characterisation of flaking or discarded paint fragments. To date, determination of metals has largely relied on analysis following sample decomposition in strong acid [8, 10-12]. This approach is rather time consuming and decomposition is often incomplete because of the poor solubility of some paint matrices under acidic conditions. Field portable X-ray fluorescence (FP-XRF) is a non-destructive, multi-element technique that has been applied to paints layers in situ in the domestic, commercial and industrial settings and for the study of cultural heritage objects [13-16]. Its application to boat paints, however, appears to be limited to a single, feasibility study in which it was proposed that ship hulls were screened for tin prior to discrimination and quantification of organotin compounds by GC-MS [17]. To this end, therefore, we describe how FP-XRF can be used to rapidly ascertain the surficial concentrations and distributions of a range of metals in fragments of spent boat paints collected from slipways, harbours, yards and abandoned boats. The XRF results are compared with those obtained using a more conventional approach (aqua regia digestion and inductively coupled plasma-mass spectrometry; ICP-MS) and are discussed in terms of the likely sources and types of paints.

2. Materials and methods

2.1. Sampling and sample locations

Paint fragments were either collected directly from boatyards, shipyards, slipways and from boats abandoned on foreshores specifically for the purposes of this study, or were obtained from samples that had been archived (and stored in the dark in an airtight polyethylene box and in individual zip-locked bags) from previous research programmes [12,18]. Sampling locations are described below and details of the number and nature of samples analysed and their dates of collection and coding are given in Table 1.

Windermere is the largest freshwater lake in England (18 km in length). It is a popular venue for leisure craft and one of only six designated inland bathing areas in England. Boats are maintained and repaired on the slipways and hardstandings of a number of designated yards and marinas. The Gannel in north Cornwall, south west England, is a small (3.7 km in length), macrotidal, ria-type estuary that became silted due to mine waste. Abandoned moorings, derelict boats and the remains of old yards attest to the historical significance of boating and shipping in the estuary. The Taw-Torridge estuaries in north Devon form a twin, macrotidal, bar-built estuarine system (with a combined length of 22 km). As well as a number of marinas and small boatyards, the system supports a fish dock, large shipyard and two Royal Marine bases, and is also a Site of Special Scientific Interest (SSSI). The River Blackwater estuary (21 km in length) is a macrotidal, coastal plain complex in East Anglia, eastern England. It is home to several marinas and boatyards and is an internationally recognised conservation area for wading birds. Pin Mill is a hamlet on the southern shore of the River Orwell estuary (20 km in length), a mesotidal, coastal plain complex in East

Anglia, and was once a busy landing point for ship-borne cargo and a centre for the repair of Thames sailing barges. The local mudflats are home to a variety of disused boats, including barges, in various states of decay. Malta is a small island in the central Mediterranean and an important transshipment hub. Here, commercial boats and ships are maintained and repaired in regulated yards but small recreational and fishing craft are often maintained along the shore, on roads and slipways and on makeshift hardstandings. Ampelakia is a small coastal town on the Greek island of Salamis. As in Malta, small boats are often maintained at unregulated sites along the coastal zone but the maintenance and repair of a variety of ships takes place in two regulated yards.

Samples of discarded paint from boat facilities, shipyards and slipways and samples of flaking paint from abandoned, derelict boats lying on the foreshore were collected using plastic tweezers and stored in individual zip-lock bags. Paint flakes from abandoned boats were collected from the hull region and, where accessible, from other parts of the vessel (e.g. deck, cabin, transom, winch, railings, nameboard).

Where several, distinct layers of paint were evident on the hull, multiple samples were retrieved accordingly. In the laboratory, samples were manually cleared of any significant, visible extraneous material (algae, shell debris, grit) and stored in individual zip lock bags in a series of polyethylene boxes at room temperature and in the dark pending analysis.

2.2. FP-XRF analysis

In X-ray fluorescence, a sample (liquid, powder, solid or film) is irradiated with X-rays that cause electrons from an inner energy orbital (K or L level) to be ejected.

Electrons from higher energy levels then fill the vacancies and excess energy is emitted in the form of X-ray photons whose wavelengths are characteristic of the elements present. Emissions are classified as K or L and as α or β depending on whether transitions from higher energy levels span one or two orbitals, respectively.

In the present study, paint fragments were analysed simultaneously for Ba, Cr, Cu, Pb, Sn and Zn by energy dispersive XRF spectrometry using a battery-powered Thermo Scientific Niton FP- (hand-held-) XRF analyser (model XL3t 950 He GOLDD+). The instrument is fitted with an X-ray tube with Ag anode target excitation source, operating at voltages up to 50 kV and at beam currents up to 200 μ A, and a geometrically optimised large area drift detector. A CCD camera stores sample images and data are transferred via USB, Bluetooth or an RS-232 serial communicator using Thermo Scientific Niton data transfer (NDT) PC software. In the present study, the instrument was placed in a bench top accessory stand for operation in the laboratory. Individual paint fragments were carefully placed in the centre of a 6 μ m polypropylene film slide using tweezers, and the slide was then placed over a 3 mm small-spot collimator above the detector. Overall measurement time was between 120 and 150 seconds and spectra up to 40 keV were quantified using a factory-installed algorithm (fundamental parameters calibration) for “plastics” mode, yielding elemental concentrations in parts per million (μ g g⁻¹) with an error of 2σ or 95% confidence. Spectra were also inspected visually in order to ascertain the significance of any interferences arising from energy peak overlaps.

By default, the centre of what appeared to be the outer (upper) face of each paint fragment was analysed. Additionally, where the face of a fragment was variable in

appearance and sufficiently large, the spatial distribution of metals was mapped, and where two or more distinct layers were evident, both the outer and inner faces were analysed. For an evaluation of precision, selected fragments were analysed, fixed in position with respect to the collimator, five times.

The instrument detection limits, supplied by the manufacturer and in $\mu\text{g g}^{-1}$ for a SiO_2 matrix analysed using the optimum (“mining”) mode and for a period of 60 seconds, are as follows: Ba = 50; Cr = 25; Cu = 12; Pb = 4; Sn = 16; Zn = 6. Triplicate measurements of a reference material that was certified for concentrations of Cr and Pb (Niton PN 180-554, polyethylene impregnated with metals; Cr = $995 \mu\text{g g}^{-1}$; Pb = $1002 \mu\text{g g}^{-1}$) returned mean (\pm one sd) concentrations of $1022 (\pm 51) \mu\text{g g}^{-1}$ and $922 (\pm 3.3) \mu\text{g g}^{-1}$, respectively. [Note that there is currently just one series of XRF paint standards that is certified on a mass basis (NIST 2569), and that certified values are restricted to relatively low concentrations (up to $300 \mu\text{g g}^{-1}$) of Pb [19].]

2.3. Digestion and ICP analysis

For comparative purposes, the total concentrations of metals in selected paint fragments were also measured (from the Blackwater and Orwell estuaries and from a yard in Ampelakia) by inductively coupled plasma-mass spectrometry (ICP-MS) after acid digestion. Thus, whole fragments of up to 0.1 g were accurately weighed into individual 24 ml Pyrex beakers to which 5 ml of aqua regia (3:1 HCl:HNO₃; both Fisher Scientific TraceMetal grade) were added. The contents of each beaker were gently boiled under watch glasses for about an hour before being allowed to cool for two hours. Digests were then transferred to individual 100 ml volumetric flasks and

diluted to mark with Millipore Milli-Q water (>18 MΩcm). Procedural controls were performed in triplicate likewise but in the absence of paint fragments.

Digests and, where necessary, dilutions thereof, were analysed for ^{136}Ba , ^{52}Cr , ^{65}Cu , ^{208}Pb , ^{118}Sn , ^{66}Zn and a range of other metals using a Thermo X-Series ICP mass spectrometer with collision cell (ThermoElemental, Winsford, UK). Samples were introduced via a concentric glass nebuliser coupled with a conical spray chamber. External calibration was achieved using 5 matrix-matched, multi-element standards and three blanks, and $50\ \mu\text{g L}^{-1}$ of both ^{115}In and ^{193}Ir were added to all standards, blanks and samples to compensate for instrumental drift and variations in plasma conditions. Metal concentrations in the digests were corrected for any contamination measured in the controls and then converted to a dry wt/wt basis.

3. Results and discussion

3.1. Analytical figures of merit for the FP-XRF and potential spectral interferences

In total, 99 paint fragments were analysed by FP-XRF in the present study and, including replicate or multiple measurements of the same sample, about 200 analyses were performed. Analytical precision, based on measures of 95% confidence or 2σ , was generally better than 15% for all metals, but often declined towards about 30% as concentrations approached the lowest values that were detectable. An alternative measure of precision was derived from multiple analyses of the same paint fragments whose positions were fixed relative to the collimator. Results revealed relative standard deviations (1σ relative to the mean) of 15% for Ba and less than 10% for Cr, Cu, Pb, Sn and Zn for a fragment sampled from an the hull of an abandoned boat on

the Gannel estuary (G8) and less than 10% for Cu, Pb, Sn and Zn in a fragment collected from a slipway in Lake Windermere (W10; Ba and Cr were not detected in this sample).

Although analysis of a reference material returned concentrations of Cr and Pb that were within 8% of certified values, it is important to assess the significance of any spectral interferences arising from a more heterogeneous, multi-element paint matrix and, therefore, limitations on the data delivered by the FP-XRF. (Note that while elements are associated with distinct fluorescence lines, the detector has resolution limitations and energy peaks have typical widths of 0.2 to 0.3 keV; [20]) To this end, we examined individual spectra arising from the analysis of 30 spent paint fragments where three or more metals were detectable. Spectra for two contrasting samples (a slipway sample from Windermere, W5, and a hull fragment from a boat abandoned on the Gannel, G7) are shown in Figure 1 to exemplify the principal fluorescence peaks and some of the interferences. Thus, for Cu there was always a distinct, interference-free peak at 8.05 keV (corresponding to the Cu-K α fluorescence line) but a secondary peak at 8.90 keV (Cu-K β) was often present on the shoulder of a Zn peak at 8.64 keV (Zn-K α). Distinct peaks for Zn were always present at 8.64 keV and 9.57 keV (Zn-K β) while for Ba there was a distinct peak at 32.19 keV (Ba-K α) but a secondary peak at 4.47 keV (Ba-L α) overlapped with Ti-K α at 4.51 keV. Regarding Pb, a distinct peak always occurred at 12.61 keV (Pb-L β), with a smaller secondary L peak at 14.76 keV (Pb-L γ); a peak also occurred at 1.55 keV (L α) and, although it exhibited some overlap with As-K α at 10.54 keV, there was no evidence for the presence of significant quantities of the metalloid in our samples from analysis of other As lines. Chromium exhibited a peak at 5.42 keV (Cr-K α) that was close to V-K β at 5.43 keV while a

second peak at 5.95 keV (Cr-K β) displayed some overlap with Mn-K α at 5.90 keV. The Sn line at 3.65 keV (Sn-L α) was generally obscured by a Ca peak at 3.69 keV (Ca- K α) but a smaller, distinct peak at 25 keV (Sn-K α) was observed when sufficient quantities of the metal were present. Subsequent analysis of paint fragment digests by ICP (see below) confirmed that Ca, Mn and Ti were present in many samples at concentrations in excess of 1000 $\mu\text{g g}^{-1}$, but that As and V were undetectable ($< 1 \mu\text{g g}^{-1}$) or were below concentrations of 10 $\mu\text{g g}^{-1}$.

In most cases, the factory-installed fundamental parameters calibration is able to confirm positive detection of an element from a single, distinct fluorescence peak, with or without corrections for other, less clear peaks. With respect to fragments of boat paints, we conclude that spectral interferences are unlikely to have a significant impact on the concentrations of Ba, Cu, Pb and Zn, but that false positives may be returned for Cr if V is present in appreciable quantities, and Sn when a secondary, higher energy peak is absent and Ca is present.

Table 2 shows the overall range of detectable concentrations encountered in the paint fragments and arising from all FP-XRF analyses. This represents an approximate working range for each metal that spans at least three orders of magnitude, although concentrations of Cr and Sn towards the lower end may be subject to some uncertainty as discussed above. Since all metals were undetectable in a number of cases, and with the exception of Cr and Sn, the lower limits reported in Table 2 may be regarded as approximate indicators of the working detection limits under the analytical conditions employed and for the matrix under investigation.

3.2. Inter-fragment variation of metal concentrations and source apportionment

Figure 2 shows the concentrations of Ba, Cr, Cu, Pb, Sn and Zn measured by FP-XRF at the centre of the outer face of each paint fragment ($n = 99$); also annotated on each panel is a statistical summary of the results. Concentrations are highly variable, both overall and for a given sampling campaign. This is perhaps not surprising since paints used on boats serve a variety of functions (e.g. priming, decoration, anticorrosion, antifouling), are a multitude of colours, and are derived from a diversity of contemporary and historical manufacturers. In general, however, the distribution and concentrations of metals measured by FP-XRF are consistent with known uses of metals in boat paints and as discussed briefly below.

The highest concentrations of Cu (in excess of 50% on a dry wt/wt basis in some cases) and Sn (up to concentrations of about 4%) were found on the lower hulls of boats or in fragments of paint retrieved from yards and slipways where hull maintenance had been taking place, reflecting the use of Cu(I)- and organotin-based biocides in contemporary and historical antifouling formulations. The more diverse distributions of Ba, Pb and Zn are consistent with the more general application or range of applications of these metals in modern and historical paints. Specifically, Ba is used as a filler and whitener as BaSO_4 , while Zn compounds are used as booster biocides (e.g. Zn pyrithione), stabilisers and absorbers of uv radiation; Zn-based compounds are also used in undercoats, blast primers and formulations that afford galvanic protection to steel hulls. Lead, although now restricted in use because of health concerns but measured at concentrations up to 20%, has been used in primers (e.g. red lead: Pb_3O_4), in interior and exterior paints to enhance drying, provide corrosion resistance or pigment for colour or opacity, in tie-coats (e.g. PbSO_4) and in

antifouling formulations as various organo-lead compounds [21]. Significantly, some products containing high concentrations of Pb still appear to be available to consumers (a primer scraped from the exterior of a recently discarded paint can from Ampelakia contained 35% Pb). Chromium was detected in the lowest number of cases ($n = 26$) but the highest concentrations (in excess of 2%) were associated with yellow or red fragments containing high concentrations of Pb and in an atomic ratio consistent with the composition of the pigment lead chromate (PbCrO_4).

3.3. Intra-fragment variability of metal concentrations

The results above have highlighted the range in absolute and relative concentrations of different metals in contemporary and historical boat paints. Also apparent from the results is that fragments arising from the same boat, or even the same region of a given boat, may be highly heterogeneous, especially if the vessel is abandoned and in a state of disrepair. This heterogeneity may arise from different types of paint shedding from different parts of the boat or from multiple layers of paint that are variably exposed on the same section. The latter effect is exemplified in Figure 3 from the FP-XRF analysis of fragments of differently coloured paints on the hull of an abandoned boat on the Taw-Torridge estuary; thus, within less than a square metre of the hull, surficial concentrations of Cr, Cu and Pb range from not detected to 31,360 $\mu\text{g g}^{-1}$, 449 to 19,510 $\mu\text{g g}^{-1}$ and 166 to 146,000 $\mu\text{g g}^{-1}$, respectively.

Because of the successive applications of paint, undertaken during a single repair or over a period of time, metals in the same fragment may also exhibit very different concentrations when the two faces are considered or even when the same face is mapped spatially. Spatial variability on an outer face may arise because the paint does

not erode or weather homogeneously, thereby exposing different quantities of the layer beneath, while variations on an inner face may reflect inconsistencies in cleaning and preparation prior to the application of a new coat of paint. With respect to the hull, for example, typical methods of cleaning, such as hand sanding, high pressure water hosing or sand blasting, tend to remove variable quantities of old paint from the substrate.

In Table 3, results of analyses of different regions of the same fragments are exemplified for samples collected from the hulls of two steel ships undergoing repair (A1 and A6) and hull paint from an abandoned wooden houseboat and winch paint from an abandoned wooden barge (B4 and B12, respectively). Regional analysis of the same face reveals variability that, in many cases, is close to or marginally greater than our precision measurements; in other cases, however (e.g. Pb and Zn in the upper faces of B4 and B12), variability is considerably greater. The former observation suggests a rather uniform paint surface while the latter is more indicative of differential erosion and weathering of the surface. With the exception of Sn and Zn in fragment A6, and where metals were detected on both faces, there was a significant difference ($p < 0.05$ according to a series of two-sample *t*-tests) between mean concentrations of the upper and lower face. In some fragments (e.g. A6), mean metal concentrations in the two faces differed by less than 30%, suggesting the layering of different formulations of the same type of paint or the differential leaching of metals from the surface and back face of the same application. In other fragments (e.g. A1), mean concentrations of some metals differed by an order of magnitude, suggesting that layers are composed of different types of paint (for example, undercoats or primers versus top coats or antifoulants).

3.4. A comparison of results from FP-XRF and ICP-MS

Selected paint fragments sampled from abandoned boats in the Blackwater and Orwell estuaries and ships undergoing repair in Ampelakia were also analysed by ICP-MS after acid digestion. A comparison of the metal concentrations in the fragments derived by FP-XRF and ICP is shown in Figure 4; note that single, total concentrations are obtained by ICP, while multiple concentrations are gained from spatial mapping by XRF (see above). Results of correlation analysis of each data set reveals relationships for Ba, Cu, Pb, Sn and Zn that are statistically significant ($p < 0.05$) and a relationship for Cr that is marginally significant ($p < 0.1$). For Cu, Pb and Zn there are approximately equal numbers of data points positioned either side of unit slope, while for Ba, Cr and Sn, more data points lie above unit slope than below.

Neither the strength of the relationship nor the closeness of the data to unit slope is necessarily indicative of the extent of disagreement between the two analytical methods. Rather, the closest correlations (Pb and Zn) appear to reflect the relatively low heterogeneity within fragments that were analysed at multiple locations by XRF. Conversely, greater scatter in the relationships exhibited by the remaining metals appears to reflect, at least partly, greater dispersion of these elements within fragments that is ascertained by FP-XRF. In the few cases where multiple measurements returned by XRF were always greater than single measurements obtained by ICP (for example, Ba, Pb and Sn in one or more fragments from Ampelakia), it is suspected that aqua regia digestion of the paint polymers may not have been complete. Visual inspection of the digests suggested that the degree of paint dissolution varied among the samples, and the results presented here suggest that

partial digestion may affect metals differently depending on the nature of their binding or incorporation into the matrix. With respect to Sn, specifically, data above unit slope may reflect organotin bound to the polymer by an ester link which would be difficult to digest in acid, although interferences in the XRF analyses arising from the presence of Ca cannot be ruled out at low concentrations below a few hundred $\mu\text{g g}^{-1}$.

3.5. Applications and advantages of FP-XRF

Fragments of boat paint represent a significant, heterogeneous source of contaminants in boatyards and on slipways where craft are maintained and repaired and in the vicinity of derelict vessels. Since finer particles of paint are highly mobile and many toxic metallic components contained therein are readily bioaccessible, paint waste is hazardous to human health and to wildlife [22,23]. Paint fragments also pose a threat to local sediment quality and, through their gradual dissolution, to both overlying and interstitial waters [2]. ICP-MS affords a sensitive means of determining the bulk metallic content of individual paint fragments following acid digestion. However, a rapid means of inspecting and screening boat paint is critical for instantaneous decision-making and an initial evaluation of the risks posed by boats in a poor state of repair or by accumulations of waste whose sources are not clear. With developments in miniaturisation of X-ray excitation sources and improved detection systems, FP-XRF has become more commercially available and more affordable over the past decade and is an attractive proposition in this respect (the capital cost of FP-XRF is typically around five times lower than that of ICP-MS; [20]). The technique requires minimal or no sample preparation and yet attains high sample throughputs (up to 30 per hour) and immediate, definitive identification of many metals without complex interpretation. Although we restricted our preliminary analyses to the laboratory, the

instrument may be readily deployed in the field provided that irradiated and secondary X-rays are adequately shielded. Discrete paint fragments would be subject to the same process and limitations described herein, while for direct, in situ analyses potential spectral and matrix interferences arising from the underlying substrate may have to be considered.

FP-XRF has particular potential in rapidly identifying metals in boat paints that have been restricted or banned and/or that are classified as priority hazardous substances under the Water Framework Directive [24]. Thus, the technique is able to detect Pb at concentrations well below a 0.5% level recommended for human safety [25] and even towards a newer standard for lead in paints for consumer products of $90 \mu\text{g g}^{-1}$ [26]; concentrations of Sn in hull paints as low as a few hundred $\mu\text{g g}^{-1}$ are detectable provided that the analysis delivers a peak at the higher energy level (25 keV; Sn- K_{α}) (or lower concentrations if significant quantities of Ca are not present). Following an initial evaluation using FP-XRF, further analyses involving sample preparatory work may be necessary for a full risk assessment. For Sn and, possibly Pb and Zn, discrimination and quantification of the precise organo- forms present by, for example, coupling gas chromatography and ICP-MS, would be desirable.

Acknowledgements

Dr Andy Fisher, UoP, is thanked for assistance with the ICP analysis. This study was funded by a Plymouth University Marine Institute grant.

References

- [1] R. Lambourne, The painting of ships. In: Paint and surface Coatings – theory and practice, ed. R. Lambourne and T.A. Strivens, Woodhead Publishing (1999), Cambridge, England, pp529-549.
- [2] A. Turner, Marine pollution from antifouling paint particles, Mar. Poll. Bull. 60 (2010), 159-171.
- [3] K.V. Thomas, M. McHugh, M. Hilton, M. Waldock, Increased persistence of antifouling paint biocides when associated with paint particles, Environ. Poll. 123 (2003) 153-161.
- [4] Y.C. Song, J.H. Woo, S.H. Park, I.S. Kim, A study of the treatment of antifouling paint waste from shipyard, Mar. Poll. Bull. 51 (2005) 1048-1053.
- [5] British Marine Federation. Environmental code of practice: Practical advice for marine businesses, sailing clubs and training centres. Egham, Surrey (2005).
- [6] DAFF, Anti-fouling and in-water cleaning guidelines, Department of Agriculture, Fisheries and Forestry (2012), Canberra, 26pp.
- [7] Singh N, Turner A. Trace metals in antifouling paint particles and their heterogeneous contamination of coastal sediments. Mar Poll Bull 2009; 58: 559-564.

- [8] A. Turner, Metal contamination of soils, sediments and dusts in the vicinity of marine leisure boat maintenance facilities, *J. Soil. Sed.* 13 (2013) 1052-1056.
- [9] C. Lord-Boring, I.J. Zelo, Z.J. Nixon, Abandoned vessels: impacts to coral reefs, seagrass, and mangroves in the US Caribbean and Pacific territories with implications for removal. *Mar. Technol. Soc. J.* 38 (2004) 26-35.
- [10] L.E. Booher LE, Lead exposure in a ship overhaul facility during paint removal, *Am. Ind. Hyg. Ass. J.* 49 (1988), 121-127.
- [11] H.C. Zedd, Y.P. Walker, J.E. Hernandez, R.J. Thomas, Lead exposures during shipboard chipping and grinding paint-removal operations, *Am. Indust. Hyg. Ass. J.* 54 (1993), 392-396.
- [12] R. Parks, M. Donnier-Marechal, P.E. Frickers, A. Turner, J.W. Readman, Antifouling biocides in discarded marine paint particles, *Mar. Poll. Bull.* 60 (2010) 1226-1230.
- [13] K. Ashley, M. Hunter, L.H. Tait, J. Dozier, J.L. Seaman, P.F. Berry, P.F., Field investigation of on-site techniques for the measurement of lead in paint films, *Field Anal. Chem. Technol.* 2 (1998) 39-50.
- [14] D.J. Kalnicky, R. Singhvi, Field portable XRF analysis of environmental samples, *J. Haz. Mat.* 83 (2001) 93-122.

- [15] X. Hou, Y. He, B.T. Jones, Recent advances in portable X-ray fluorescence spectrometry, *Appl. Spec. Rev.* 39 (2004), 1-25.
- [16] I. Sianoudis, E. Drakaki, A. Hein, Educational X-ray experiments and XRF measurements with a portable setup adapted for the characterization of cultural heritage objects, *Eur. J. Phys.* 31 (2010) 419-431.
- [17] T. Senda, O. Miyata, T. Kihara, Y. Yamada, Inspection method for the identification of TBT-containing antifouling paints, *Biofouling* 19 (2003) 231-237.
- [18] A. Turner A, N. Singh N, J.P. Richards, Bioaccessibility of metals in soils and dusts contaminated by marine antifouling paint particles, *Environ. Poll.* 157 (2009) 1526-1532.
- [19] J.L. Molloy, J.R. Sieber, K.E. Murphy, S.E. Long, S.D. Leigh, Certification of NIST SRM 2569 lead paint films for children's products, *X-Ray Spec.* 41 (2012) 374-383.
- [20] P.T. Palmer, R. Jacobs, P.E. Baker, K. Ferguson, S. Webber, Use of field-portable XRF analyzers for rapid screening of toxic elements in FDA-regulated products. *J. Agric. Food Chem.* 57 (2009) 2605-2613.
- [21] I. Omae, Organotin antifouling paints and their alternatives. *Appl. Organomet. Chem.* 17 (2003) 81-105.

[22] I. Links, K.E. van der Jagt, Y. Christopher, M. Lurvink, J. Schinkel, E. Tielemans, J.J. van Hemmen, Occupational exposure during application and removal of antifouling paints. *Ann. Occup. Hyg.* 51 (2007) 207-218.

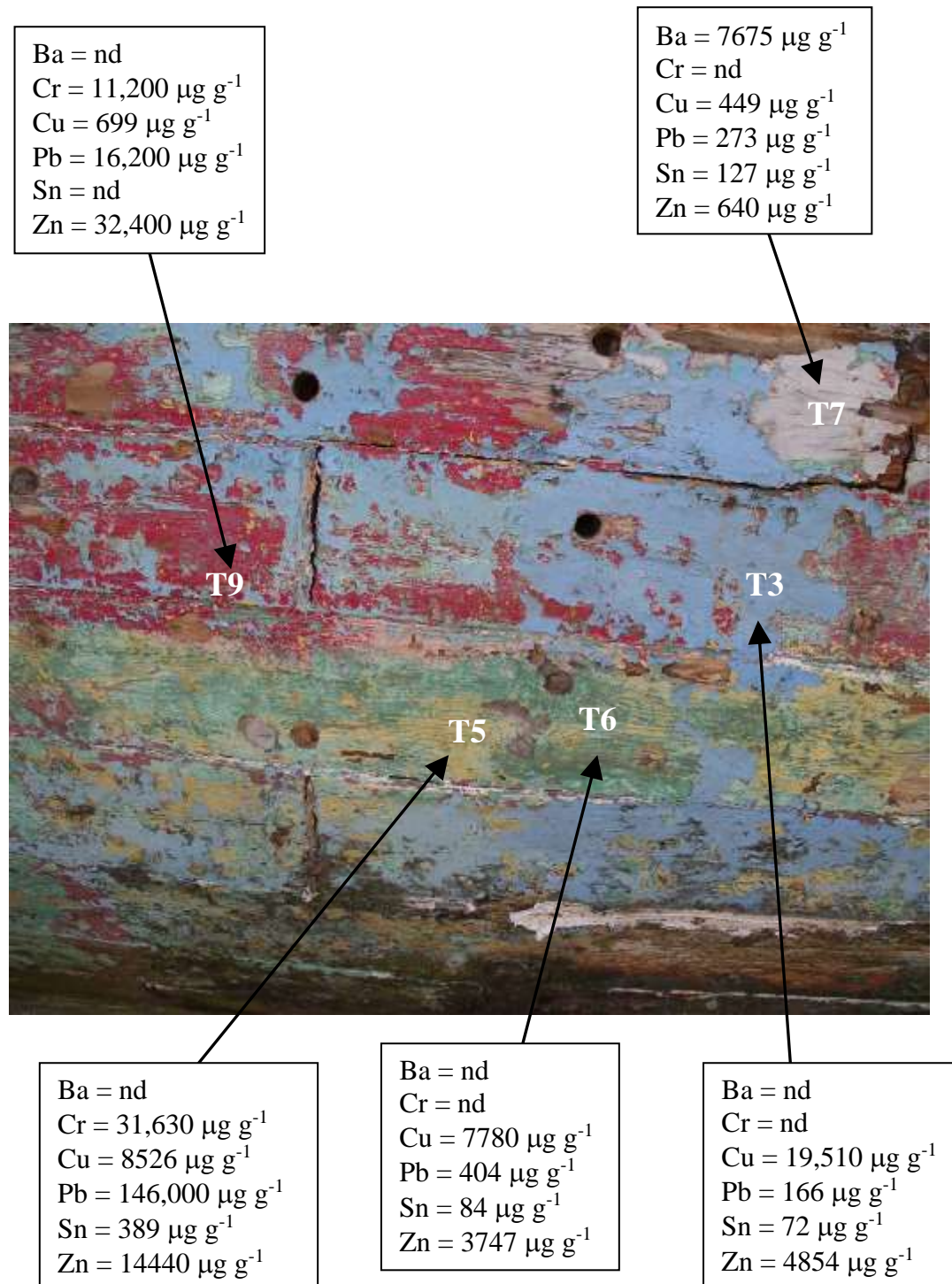
[23] A. Turner, J. Hambling, Bioaccessibility of trace metals in sediment, macroalgae and antifouling paint to the wild mute swan, *Cygnus olor*, *Wat .Air. Soil Poll.* 223 (2012) 2503-2509.

[24] EU Directive, 2013/39/EU of the European Parliament and of the council amending Directives 2000/60/EC and 2008/105/EC as regards priority substances in the field of water policy (2013), 12.8.2013. 2011/0429 (COD).

[25] J.M. Horner, Lead poisoning from paint – still a potential problem. *J. Royal Soc. Health* 114 (1994) 245-247.

[26] D. Cobb, D., Study on the effectiveness, precision, and reliability of X-ray fluorescence spectrometry and other alternative methods for measuring lead in paints, Consumer Product Safety Commission (2009), Gaithersburg MD, 30pp.

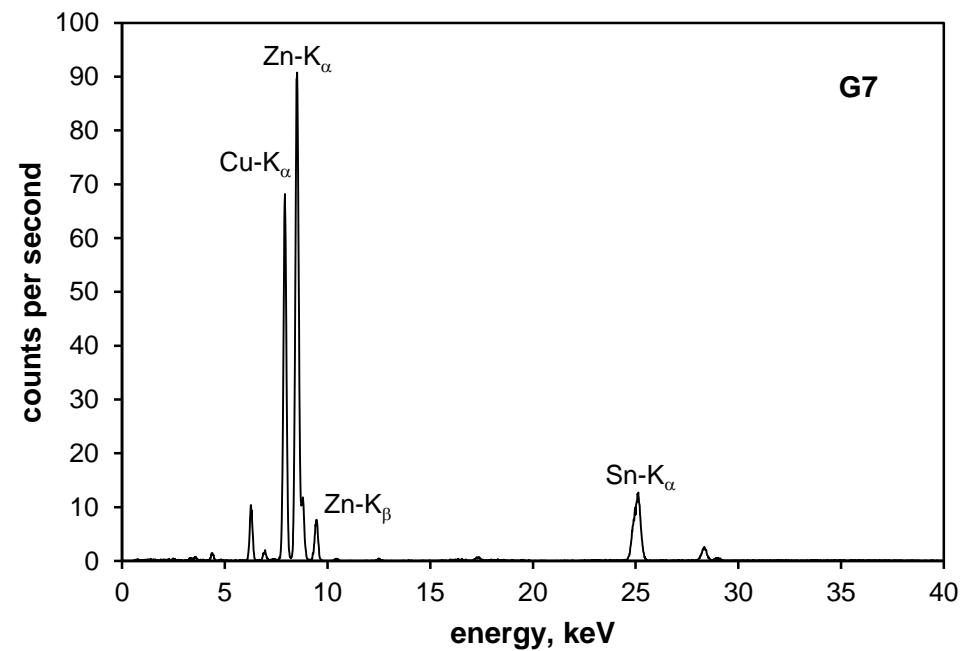
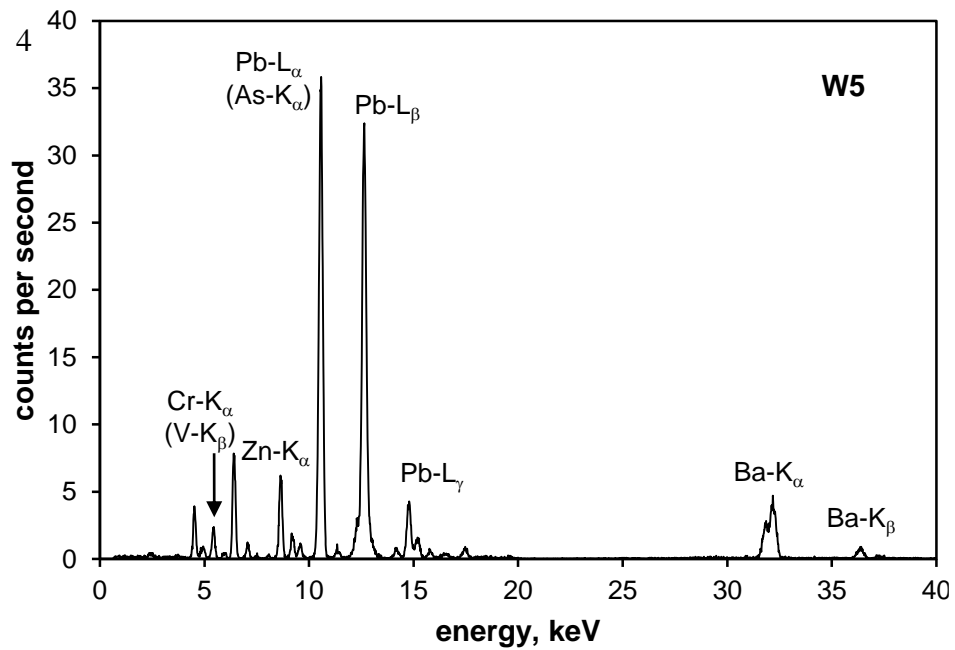
Figure 3: Distribution of metals in paint fragments collected from a section of hull of an abandoned wooden boat lying on the sandy foreshore of the Taw-Torridge estuary. [Colour on Web, b and w in print].



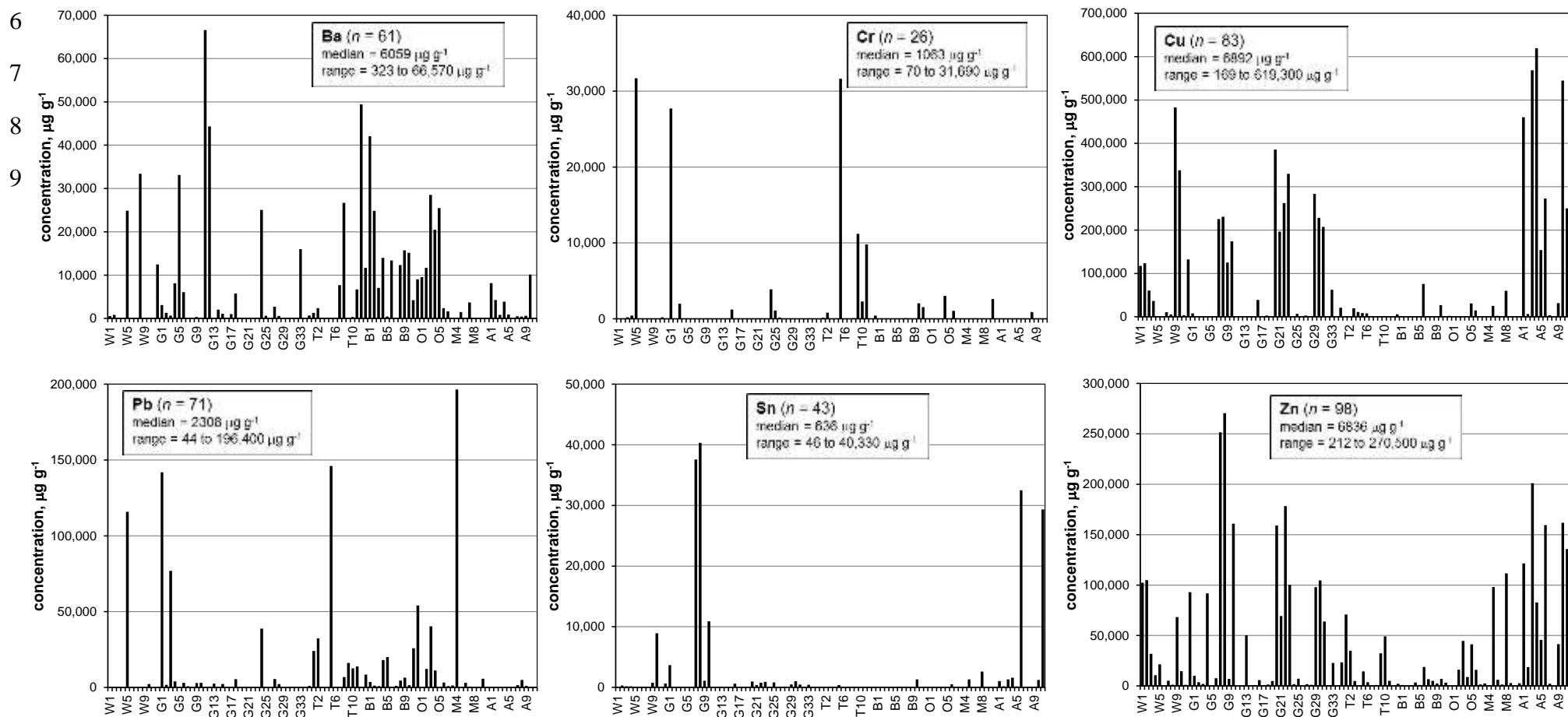
1 Figure 1: XRF spectra for samples W5 and G7, illustrating the principal peaks of interest and, in parentheses, potentially interfering peaks.

2

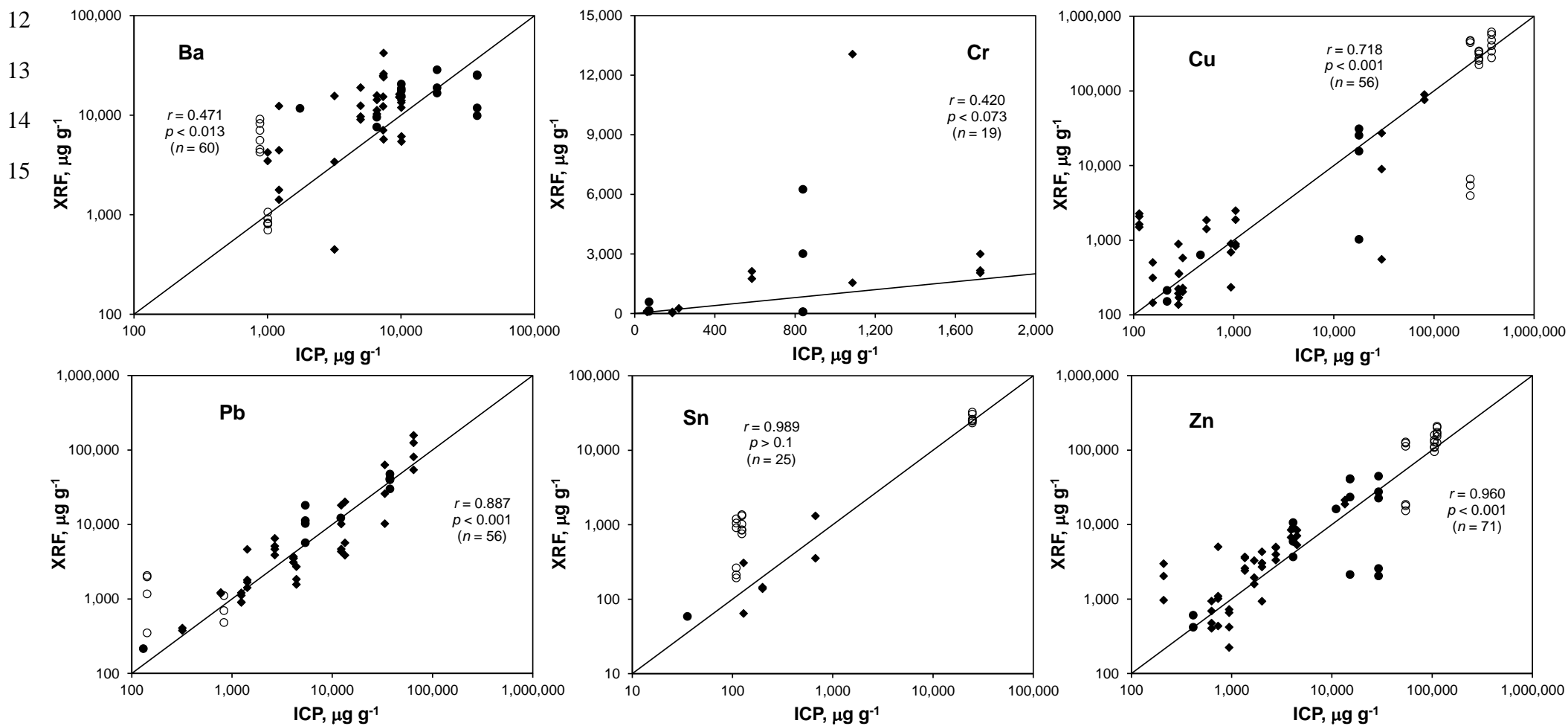
3



5 Figure 2: “Default” concentrations of metals measured in the centre of the upper face of each paint fragment ($n = 99$).



10 Figure 4: A comparison of the concentrations of metals in paint fragments derived from XRF analysis and ICP analysis following acid digestion (◆,
 11 Blackwater; ●, Orwell; ○, Ampelakia). The solid lines represent unit slope and statistical summaries are for correlation analysis of each dataset.



16 Table 1: Location and origin of the paint fragments collected for the study.

17

18 location date origin sample code no. XRF analyses

19 (no. samples)

20

21	Gannel estuary	6/12	abandoned boats on sandy foreshore	G1-G18 (18)	18
22			public slipway to foreshore	G19-G35 (16)	16
23	Taw-Torridge estuary	6/12	abandoned boats on sandy foreshore	T1-T13 (13)	13
24	Blackwater	2/13	abandoned boats on intertidal mudflats	B1-B13 (13)	37
25	Pin Mill, Orwell	2/13	abandoned boats on intertidal mudflats	O1-O5 (5)	16
26	Lake Windermere	4/08	boatyard slipways to lake	W1-W12 (12)	28
27	Malta	4/09	boatyards and slipways	M1-M11 (11)	19
28	Ampelakia	12/12	shipyards	A1-A11 (11)	46

29

30

31 Table 2: Minimum and maximum concentrations of metals determined by FP-XRF analysis of the paint fragments (193 analyses of 99 samples). Also shown
 32 is the number of cases in which elements were detected.

33

34		Ba	Cr	Cu	Pb	Sn	Zn
35							
36	minimum, $\mu\text{g g}^{-1}$ (sample code)	135 (A8)	32 (B8)	137 (B8)	39 (A10)	37 (A1)	83 (A8)
37	maximum, $\mu\text{g g}^{-1}$ (sample code)	66,600 (P1)	31,690 (W5)	619,300 (P1)	196,400 (M4)	40,330 (G8)	270,500 (P1)
38	number detected	124	50	167	137	99	193
39							

40 Table 3: Concentrations of metals in the upper and lower faces of the same paint fragments collected from abandoned boats or vessels undergoing repair (the mean
 41 and standard deviation arising from three measurements of each face is given; nd = not detected in at least one of the measurements).

43 Sample	Ba	Cr	Cu	Pb	Sn	Zn
45 A1, hull paint (steel ferry undergoing repair)						
46 upper face	8135±1064	nd	460,000±16,600	nd	1050±146	121,400±8067
47 lower face	4785±703	nd	5326±1338	nd	222±36	17,260±1789
48 A6, hull paint (steel ship undergoing repair)						
49 upper face	nd	nd	250,300±25,000	nd	29,340±3816	135,600±24,350
50 lower face	nd	nd	328,600±15,270	nd	24,600±1430	110,100±16,520
51 B4, hull paint (abandoned wooden houseboat)						
52 upper face	14,550±818	nd	nd	14,090±5648	nd	3642±456
53 lower face	5769±491	nd	nd	4493±244	nd	4937±81
54 B12, winch paint (abandoned wooden barge)						
55 upper face	9358±452	nd	2171±132	67,320±18,710	nd	321±138
56 lower face	15,660±4597	1936±267	1560±96	140,700±23,163	nd	688±50

